REPORT DOCUMENTATION PAGE

Form Approved
OMB No. 0704-0188

PLEASE DO NOT RETURN YOUR FORM TO THE ABOVE ADDRESS.

1. REPORT DATE *(DD-MM-YYYY)*	2. REPORT DATE	3. DATES COVERED *(From - To)*
15-00-2006	Final Technical Report	06/01/03 - 07/31/06

4. TITLE AND SUBTITLE
TeraHertz Nanodevices for Communication, Imaging, Sensing and Ranging

5a. CONTRACT NUMBER
F49620-03-1-0380

5b. GRANT NUMBER

5c. PROGRAM ELEMENT NUMBER

6. AUTHOR(S)
Dr. James Kolodzey
Dr. Keith Goossen

5d. PROJECT NUMBER

5e. TASK NUMBER

5f. WORK UNIT NUMBER

7. PERFORMING ORGANIZATION NAME(S) AND ADDRESS(ES)
James Kolodzey
Department of Electrical and Computer Engineering,
140 Evans Hall
University of Delaware, Newark DE, USA 19716-3130

8. PERFORMING ORGANIZATION REPORT NUMBER
ELEG332147

9. SPONSORING/MONITORING AGENCY NAME(S) AND ADDRESS(ES)
Gernot S. Pomrenke, PhD
AFOSR Program Manager - Optoelectronics and Nanotechnology
Directorate of Physics and Electronics
Air Force Office of Scientific Research; Ballston Common Towers III
4015 Wilson Blvd, Room 713
Arlington VA 22203-1954

10. SPONSOR/MONITOR'S ACRONYM(S)
AFOSR

11. SPONSORING/MONITORING AGENCY REPORT NUMBER

12. DISTRIBUTION AVAILABILITY STATEMENT
Public Availability, Distribution Unlimited

AFRL-SR-AR-TR-07-0194

13. SUPPLEMENTARY NOTES

14. ABSTRACT
This research program focused on the design, fabrication and optimization of THz devices using Group IV semiconductor nanotechnology. The devices were based on SiGe quantum wells (QWs), by intracenter transitions in doped nanostructures and photonic crystals fabricated by MBE and CVD. The SiGe QWs gave good performance, but the output powers were low and the operating temperature needed to be cryogenic. The dopant emitters were simpler in design, but the initial devices needed low temperatures so that the dopant states are occupied (carrier freeze out). With deep energy dopants, such as nitrogen in SiC, however, the emission occurs at relatively high temperatures, up to 150 K. We have demonstrated the operation of very high performance with the emitted power near 1 mW from a device several square mm in surface area.

15. SUBJECT TERMS
terahertz devices, nanotechnology, SiGe quantum wells

16. SECURITY CLASSIFICATION OF:			17. LIMITATION OF ABSTRACT	18. NUMBER OF PAGES	19a. NAME OF RESPONSIBLE PERSON
a. REPORT	b. ABSTRACT	c. THIS PAGE		32	James Kolodzey
					19b. TELEPONE NUMBER *(Include area code)* 302-831-1164

Terahertz Nanodevices for Communication, Imaging, Sensing and Ranging

Final Report to the AFOSR for the period from the start date of 6/1/03 to the end date of 7/31/06

by James Kolodzey and Keith Goossen, December 2006
Dept. of Elec. & Comp. Eng.
University of Delaware, Newark DE, USA 19716-3130
302-831-1164; kolodzey@ee.udel.edu; http://www.ee.udel.edu/~kolodzey

Air Force program: F49620-03-1-0380
Start date: 6/1/03; End date: 7/31/06

1. Cover Sheet:

program manager:
Dr. Gernot S. Pomrenke
AFOSR Program Manager - Optoelectronics, THz and Nanotechnology
AFOSR/NE
Directorate of Physics and Electronics
Air Force Office of Scientific Research
Ballston Common Towers III
4015 Wilson Blvd, Room 713
Arlington, VA 22203-1954
e-mail: gernot.pomrenke@afosr.af.mil
Tel: 703-696-8426
Fax: 703-696-8481
Room 713 mail

2. Objectives:

Develop, fabricate and characterize terahertz devices, arrays and components for integrated chip-based systems, based on SiGe nanostructures, for applications in imaging, sensing and ranging.

3. Status of effort:

This research program focused on the design, fabrication and optimization of THz devices using Group IV semiconductor nanotechnology. The devices were based on SiGe quantum wells (QWs), by intracenter transitions in doped nanostructures and photonic crystals fabricated by MBE and CVD. The SiGe QWs gave good performance, but the output powers were low and the operating temperature needed to be cryogenic. The dopant emitters were simpler in design, but the initial devices needed low temperatures so that the dopant states are occupied (carrier freeze out). With deep energy dopants, such as nitrogen in SiC, however, the emission occurs at relatively high temperatures, up to 150 K. We have demonstrated the operation of very high performance with the emitted power near 1 mW from a device several square mm in surface area. Our goal was to obtain a Group IV THz laser, which may have already been achieved using a designs provided by our Russian collaborators, but more measurements are needed to prove this. Quantum well and dopant structures were also designed to operate as THz detectors. To investigate system applications, we investigated detector HgCdTe arrays. We collaborated with Tom Allik of the SAIC organization at the Army Night Vision Lab, who loaned us a Stirling cooler and a bolometer focal plane array. With Irina Yassievich and Miron Kagan in Russia, we fabricated devices that appear to produce THz lasing. We prototyped imaging systems using focal plane arrays that operate at room temperature, based on pyroelectric detectors and bolometers. We explored the propagation of THz through materials including drywall, and modeled the underlying mechanisms. To achieve an electrically alterable photonic crystal, we built a *p-i-n* device structure and have begun its characterization. During the course of this project we have endeavored to increase the output power and operating temperature of the emitters; to make a laser by combining gain regions and resonators, to make photonic crystal structures for couplers and resonators, and explored imaging using portable devices.

4. Accomplishments/New Findings:

Accomplishments over the past three years: (a) Demonstrated the operation of THz sources, detectors, photonic arrays, and imaging with high performance devices based on SiGe, SiC and GaAs; (b) Provided data on the variety of powers, frequencies, gains, and temperatures that can be achieved from dopant based THz sources, which are needed to achieve our overarching goal of a silicon compatible THz laser; (c) Achieved THz emission output power of 180 microwatts (4.5

milliWatt/cm2) at 9 THz from silicon carbide dopant based devices with operating temperatures to 150 K (APL 87, 241114, 2005); (d) Fabricated devices that emit from 3 to 9 THz using two new materials: SiGe and GaAs and the THz mechanism was intracenter transitions in dopants at low temperatures; (e) demonstrated the appearance of new emission lines from Ga in silicon (APL, 85, 3660, 2004), and boron in silicon (unpublished); (f) A Terahertz detector based on doped silicon was fabricated and measured; (g) demonstrated that Si:Ga THz emitters and sensitive longwave HgCdTe 1-dimensional detector arrays HgCdTe that can be operated at 77K for a prototype active imaging system; (h) Achieved THz imaging with room temperature THz bolometer focal plane arrays; (i) developed new cyclic reactive etching techniques and fabricated photonic crystal resonators; (j) measured the transmission of THz though nanostructures and materials and modeled THz propagation by photon diffusion.

Problems/ challenges: we may have achieved lasing in resonant state SiGe devices, but we need a better understand of the impurity operating mechanism to achieve higher gain, and for a resonator with higher Q factor

Payoff: These results indicated the directions of research and technical approaches that can enable THz systems compatible with silicon technology and that can be investigated with DOD Lab collaboration

Suggestions for Future Work: optimize the device design for high gain; combine the active gain region with a resonator to demonstrate lasing.

4.1 THz Sources

THz Quantum Cascade Emission from SiGe Quantum Wells

Our initial approach was to obtain THz emission from quantum cascade structures based on SiGe quantum wells fabricated by molecular beam epitaxy. During the course of the SiGe quantum well project, it was observed that the emission from intracenter transitions in dopants gave significant power without the need for the epitaxial growth of quantum wells. Our plan was to optimize electrically pumped THz emitters by increasing the emitted power and increasing the operating temperature. Devices based on several operating mechanisms were designed and fabricated as shown in Fig. 1. The limitation of SiGe quantum well-based devices is that there is still no laser. A laser would have much higher powers than the present LED mode devices. Our plan to reach a laser was to optimize the design of the active region to increase the power and operating temperature, and to incorporate them in feedback resonators.

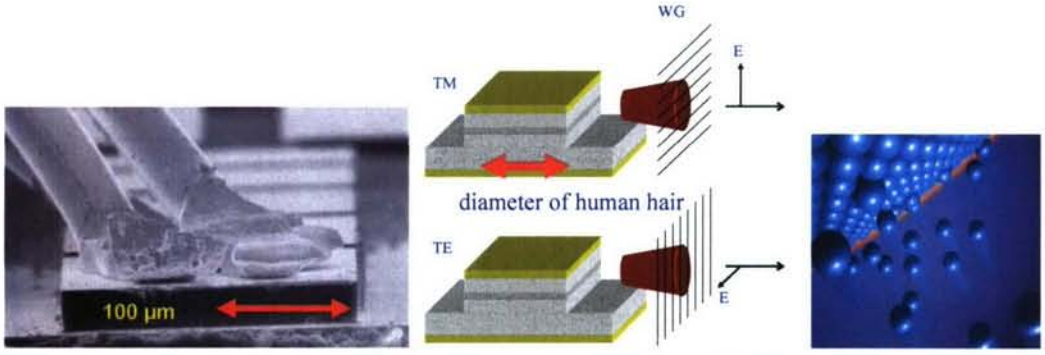

Figure 1. Left panel shows SEM micrograph of fabricated doped silicon THz emitter showing an etched mesa and gold wires. Middle panel shows illustration of THz emission beam pattern from edge emitting device. Right panel shows a stylized diagram of the molecular beam epitaxy growth.

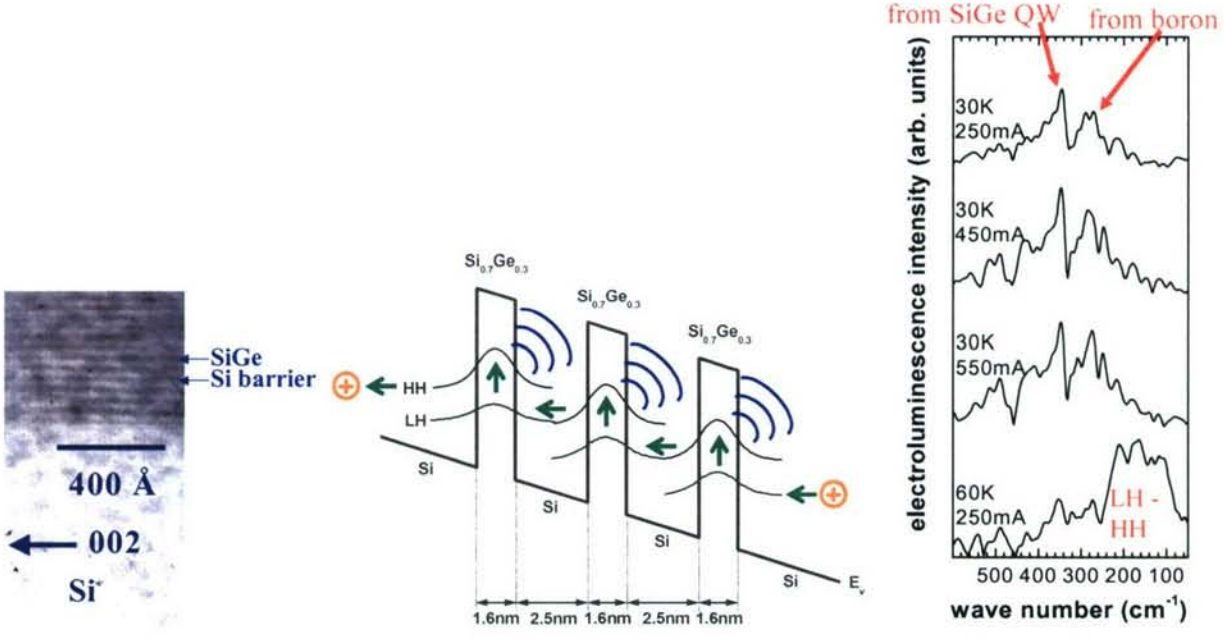

Figure 2. Terahertz emission from SiGe Quantum Cascade Structures. Left panel shows a TEM micrograph of SiGe layers fabricated at UD by the MBE technique. Middle panel shows valance band energy diagram of quantum wells under bias, illustrating cascade hole transitions. Right panel shows the spectral output near 10 THz from SiGe quantum wells at several μW peak power, which is about 100x higher power than that achieved by other SiGe groups. Also indicated is the emission line from the boron dopant transitions.

THz emission by the electrical pumping of impurities

We discovered that hydrogenic energy states of dopants produce radiative transitions in the THz range. For instance, the diagrams in figure 4 shows the energy states of the acceptors and donors, and the corresponding transitions at THz frequencies. At low temperatures below the freeze-out of mobile

carriers, the dopant atoms are in the ground state and are electrically neutral. The electrons and holes can be excited to their corresponding energy band by impact ionization from an applied current. After recapture, the carriers relax to the ground state by nonradiative acoustic phonon emission for transitions between states that are closely spaced in energy; and by radiative THz emission for states that are separated by more than the acoustic phonon energy (a few meV). These later transitions are responsible for the observed THz operation.

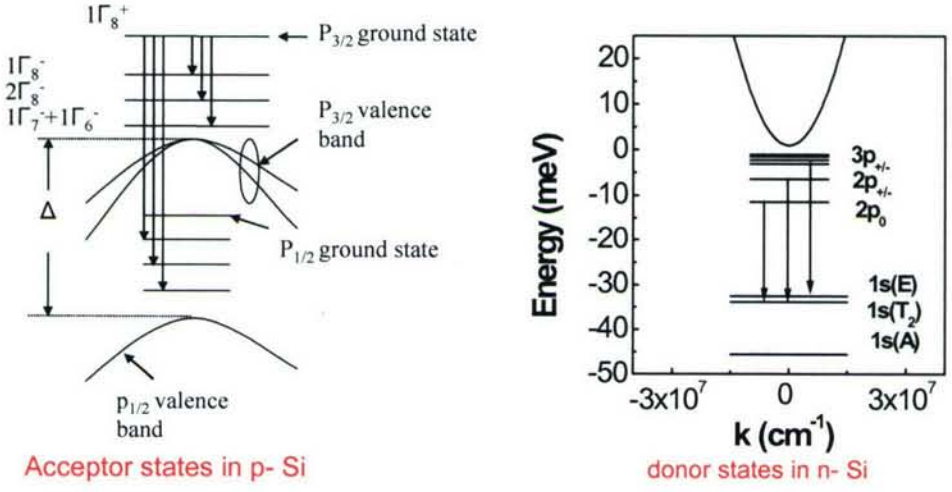

Figure 3. Hydrogenic energy levels of dopants in silicon. Left panel shows a generic energy diagram for acceptors in Si. Electron energy is positive upward. The J=3/2 band is for the heavy holes (m_j = 3/2) and light holes (m_j = ½), and the J=1/2 band is the split off band. Right panel shows the energy diagram for donors in Si. The 1s ground state is split by intervalley scattering.

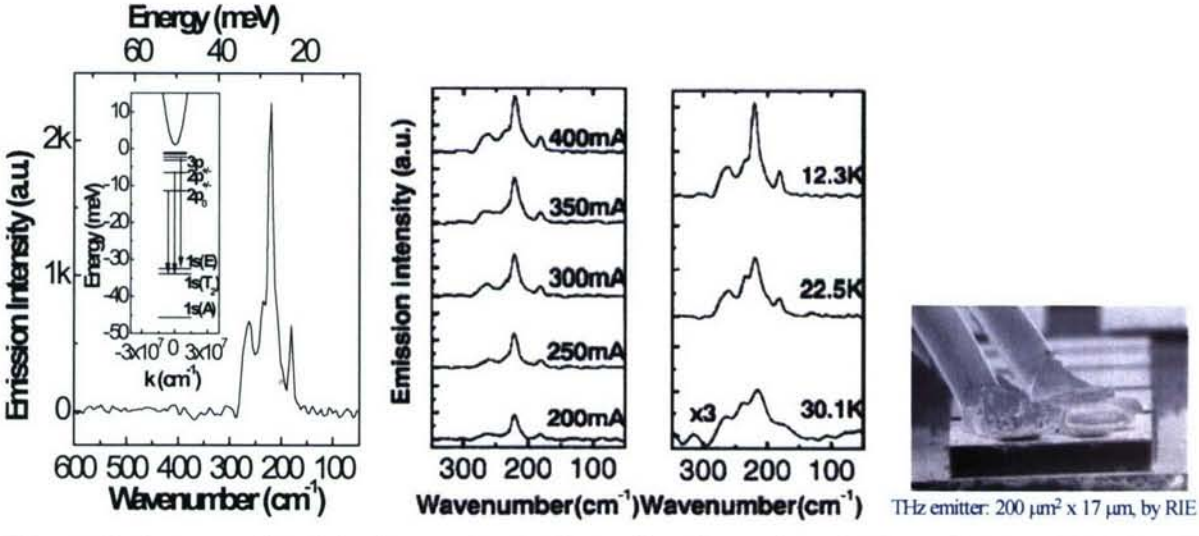

Figure 4. An example of Terahertz emission from phosphorus doped silicon devices. Left plot shows Terahertz spectrum and level scheme for phosphorus doped n-type emitter. Middle and right plots show the Terahertz emission spectrum versus current and temperature, respectively. Right panel shows SEM micrograph of fabricated mesa device.

Emission was obtained from boron and gallium doped p-type devices, with slightly different THz frequencies (Lv, Goossen & Kolodzey APL, 85, 3660, Oct. 2004), and also n-type phosphorus doped devices. These devices have simple fabrication methods and yield high output power. (conversion between different terahertz units: (100 cm^{-1} ~ 100 μm ~ 3 THz ~ 12.3 meV).

To increase the emitted power from our devices, a new series of top surface emitters was fabricated as shown in Fig. 5. Larger area emission gives higher net powers, and allows easier alignment to external optics. In addition to the emission from doped Si, emission was also obtained in the range from 1 to 3 THz from GaAs devices that were doped with silicon donors.

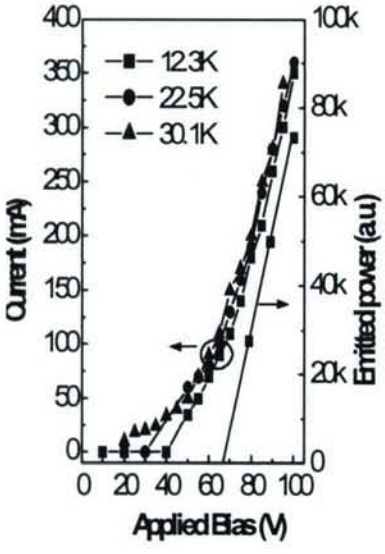

Figure 5. Current and power versus voltage for phosphorus doped Terahertz emitting device. Peak power is 120 microwatts from 4 side facets, higher than other Si-based sources; showing remarkable agreement with dopant intra-center transitions: (Lv & Kolodzey, APL, 84, 22-24, July 2004).

To extend the investigation of alternative materials, doped SiGe layers were obtained from Prof. Gene Fitzgerald of MIT. We plan to investigate THz emission from SiGe alloys, and to determine the efficiency, emission frequency, and operating temperature as a function of alloy composition. Discussion were begun with Prof. Mark Johnson at NC State to obtain GaN materials for THz devices.

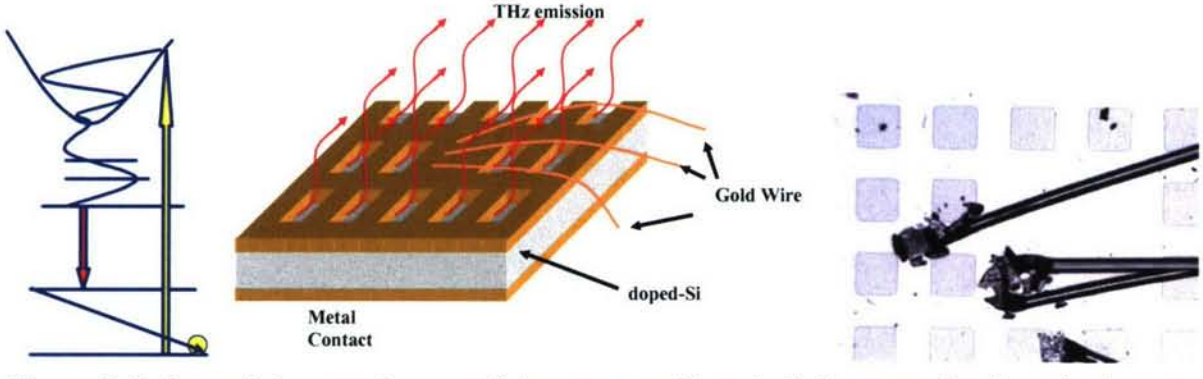

Figure 6. Left panel shows a diagram of electron transitions including pumping from the donor states to conduction band (heavy upward arrow), acoustic phonon relaxation (sloped curves and arrows), and THz radiative transition downward vertical red arrow. Middle panel shows a drawing of a surface emitter. Right panel shows a micrograph of the top view of a device with emitting silicon regions (darker squares) and wire bonds (dark rods) to the metal contacts (light continuous mesh).

To improve the device operating characteristics, several analytical models for the emission were

developed. First, an empirical model expresses the emitted power (P) versus the applied current density (J), doping concentration (N), device volume (V), and the activation energy (E_a) of excited states:

$$P \approx \eta_{ext} VN \left(AJ - \left(B_1 + B_2 e^{-\frac{E_a}{kT}} \right) J^2 \right)$$

doping current

The phosphorus doped device has an external quantum efficiency η_{ext} = 0.2 % (photons/electron). The electrical wall plug efficiency, however, is only 10^{-6} for these preliminary devices. We emphasize that the optimum doping density has not yet been determined and is still under investigation. It is unlikely that the performance cannot be significantly improved by further study. To determine the optimum doping, we are obtaining samples with a range of doping concentrations and will compare the output powers and operating temperatures.

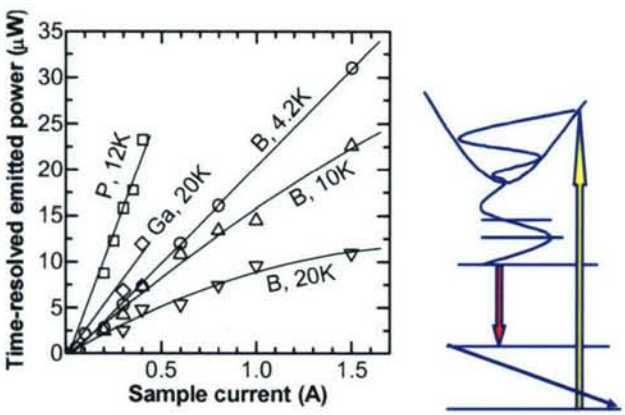

Figure 7. Comparison of Terahertz emission from several doped silicon devices. Left plot shows peak time resolved output powers from a single side emitting facet of several THz emitting devices at different operating temperatures. Right panel show concept to achieve population inversion in doped Si due to fast depopulation of ground state and a four level scheme. The upward arrow shows the electron pumping transition; the downward vertical arrow shows the lasing transition, followed by nonradiative relaxation to ground state.

A more complex model of the distribution of holes within the excited dopant states was developed and compared with experiments. Hole concentrations in excited states were calculated under various pumping rates. (JAP 98, 093710, 2005). At a fixed temperature, the hole concentrations in each excited state increased linearly with pumping current. For acceptors, the increase was faster for the lower energy $1\Gamma_8$- state than other excited states. At a fixed pumping current, hole concentrations in excited state decreased with temperature, but at a slower rate for the deeper energy states (farthest from the valence band edge). These results may be useful for designing and understanding the temperature performance of terahertz emitters based on dopant intra-center transitions. To achieve

THz emission at higher temperature, it would be best to use dopants that have a strong oscillator strength from the lowest energy excited state. The increase in hole population with current suggests that the THz emission did not saturate, so that more output power may be possible with higher pumping current. The THz emission measurements yielded new information a bout the physics of energy levels in dopants.

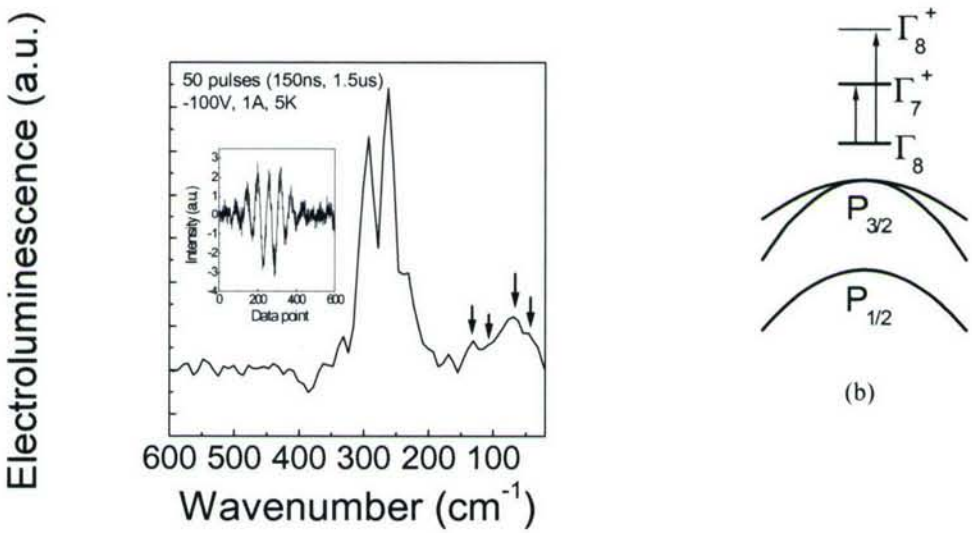

(a) (b)

Figure 8. The electroluminescence spectrum from a Boron doped silicon terahertz emitter at 5K. Four emission peaks were observed around 100 cm-1, which may be due to the impurity intra- center transitions to the ground state associated with the SO band. The inset shows the corresponding interferogram. These lines near 100 cm^{-1} are attributed to the transitions from the Γ_8 excited states to the Γ_7^+ ground state of the split-off $P_{1/2}$ band.

Terahertz emission from nitrogen doped 4H- SiC that operates at temperature of 150 K

Emission near 9 THz was produced from n-type 4H-silicon carbide doped with nitrogen. The operating temperatures were up to 150 K, higher than any silicon based THz source. The high temperature operation is attributed to the deep ionization energy level of the dopants. The 4H-SiC wafer were provided by Adrian Powell of Cree Research.

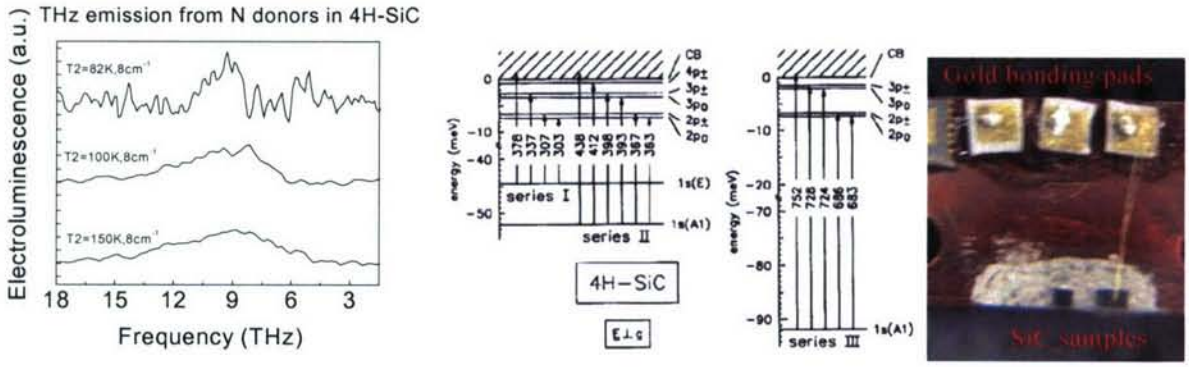

Figure 9. An example of Terahertz emission from n-type doped 4H-silicon carbide devices. Left plot shows Terahertz emission spectrum at temperatures from 82 K to 150 K with peak at 9 THz, showing that dopant based SiC emitters can operate above liquid nitrogen temperatures so that they can be cooled by portable Peltier effect thermoelectric coolers. Middle panel shows the energy level scheme of nitrogen donors in SiC, [Gotz, JAP, v. 73, 3332, 1993]. The series I and II transitions are in agreement with observed THz emission. Right panel shows photograph of SiC THz emitter chips (bottom) mounted on Cu heat sink, and wire bonded to gold plated ceramic pads.

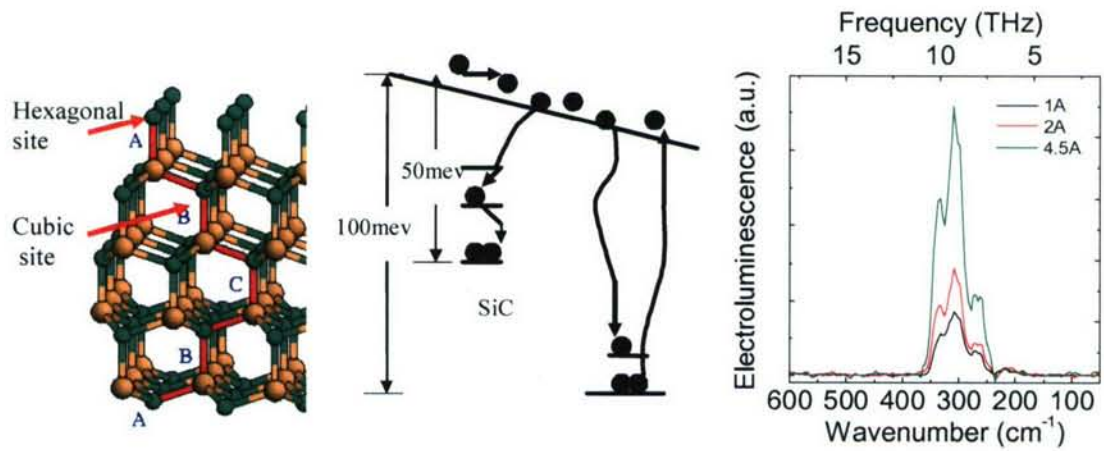

Figure 10. THz emissions from n-type 4H-SiC. Left panel shows cubic and hexagonal sites in hexagonal 4H-SiC, with different energies. Middle panel shows energy levels of nitrogen donors in 4H-SiC, with the 2 kinds of sites: hexagonal (shallow sites to left) and cubic (deeper sites to right). Right panel shows an emission spectrum at peak pulsed currents of 1, 2 and 4.5 amps, at a temperature of 4K.

We designed, fabricated, tested, and optimized an electrically pumped THz source that emits at 9 THz with a maximum operating temperature of 150 K, based on dopant transitions in nitrogen donors in the 4H hexagonal polytype of silicon carbide (APL 87, 241114, 2005). Photolithography was used to pattern topside electrical contacts with an area filling factor of 50%, using the full wafer for the bottom contact. Metal contacts were formed by the e-beam evaporation of Ti/Au layers of thickness 20/500 nm.

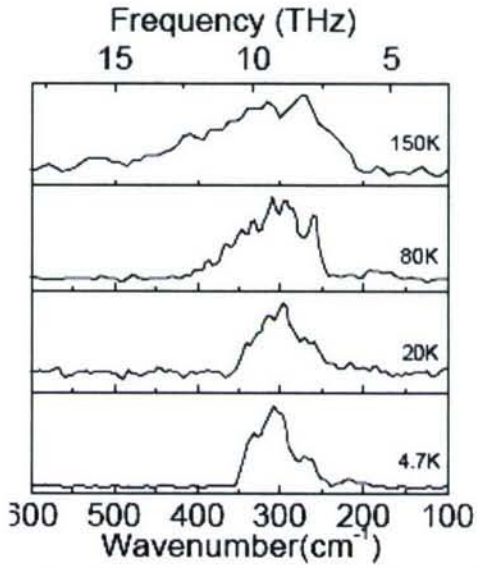

Figure 11. The dependence of THz emission on temperature for nitrogen doped 4H-SiC devices with a pumping current of 2 A. The devices were fabricated from 250 μm-thick 4H-SiC wafers with net nitrogen donor concentration $N_D - N_A = 5E17\ cm^{-3}$.

Even at room temperature, some electrons still occupy the deeper cubic site. As the temperature increased, the emission spectrum broadened, but peaks were still discernable up to 150 K, as in Fig. 11. At higher temperatures fewer electrons were available in the donor states for radiative transitions even at the deeper cubic site. The SiC devices have a relatively high radiative efficiency (10^{-3} photons per injected electron). At a pumping current of 4.7A at 4K, the integrated spectral output power was 0.18 milliWatt from the top surface with an area of 4 mm^2, which is higher than from any other group IV based THz source. Terahertz emission from silicon carbide has not been previously observed, and the results suggest that this new family of compact electrically pumped devices can be fabricated by simple processing and are suitable for low cost, practical applications.

Resonant State THz Source

We fabricated resonant state laser (RSL) devices with active boron delta doped planes located within SiGe strained layers by MBE on n-type Si substrates as shown in Fig 13. Using FTIR spectroscopy, we observed intense THz emission with wavelengths near 100 microns (3 THz) under a strong pulsed electric field. The periodicity of the measured spectral modes suggested stimulated emission. The origin of the THz emission was attributed to intra-center optical transitions between resonant states within the valence band and localized boron levels in the forbidden gap similar to that observed in compressed p-Ge.

Acceptor-doped $Si_{1-x}Ge_x$ is very attractive for fabricating the RSLs because of its good thermal properties, low absorption in the THz range, well established, relatively cheap technology, as well as the possible integration with Si-based electronics. Our group is the only one in the world presently fabricating these structures from SiGe alloys. To improve the performance of resonant state lasers developed with I. Yassievich and M. Kagan in Russia, we are growing a new series of delta doped SiGe samples by molecular beam epitaxy. Our approach is to use a thicker cap layer to prevent the depletion of carriers at the surface which may be limiting the emitted power.

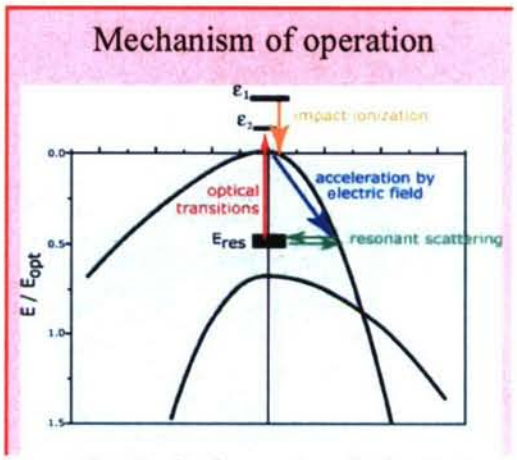

Figure 12. Excitation and emission hole transitions for boron dopants in valence band of strained SiGe, for resonant state laser (RSL). Upper level is E_{res}, and lower level is E_2. (Hole energy is positive downward).

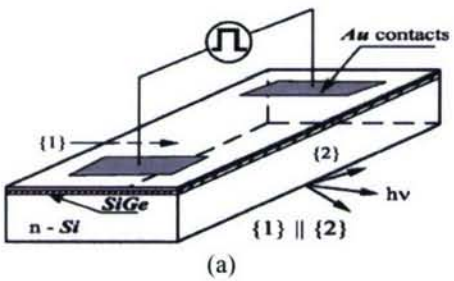

(a)

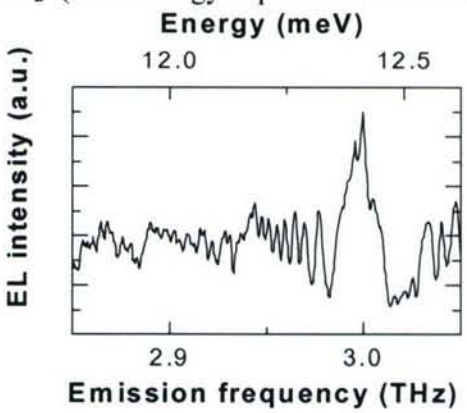

(b)

Figure 13. An example of SiGe quantum well resonant state Terahertz emitters: (left) Device rectangular resonator structure. (right) Emission spectrum showing peak near 3 THz from sample SGC399, immersed in liquid helium.

Recently, we fabricated devices that emit from 3 to 9 THz using two new materials: SiGe and GaAs. The THz mechanism was intracenter transitions in dopants at low temperatures. This work describes the THz device characteristics and limitations.

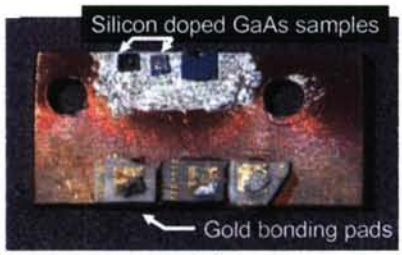

(a)

(b)

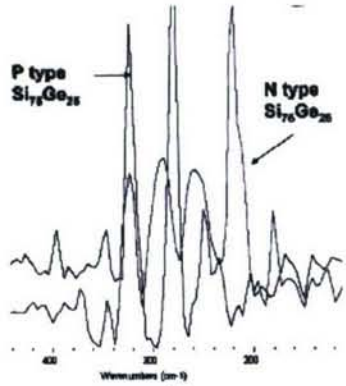

(c)

Figure 14. THz emission from using two new materials: GaAs and SiGe. Left panel shows the top view of GaAs THz sources mounted onto a copper block (2cmx4cm) for measuring.. Middle panel shows a Spectrum from GaAs THz source showing broad emission peak at 3 THz (100 cm^{-1}). Right panel shows a Strong THz output spectra from two SiGe devices. The n-type emits at 6.6 THz, and the p-type at 8.4 THz.

Portable Terahertz Sources and Coolers

Peltier effect thermoelectric coolers can achieve a cooling range of about 40 K per stage, so that a 3-stage cooler can reach a differential of about 120 K below room temperature, or about 180 K absolute. To reach even lower temperatures near 77 K, we have borrowed a Stirling cycle cooler from Dr. Tom Allik of the Army Night Vision Laboratory (Ft. Belvoir), and are developing a technique to mount a SiC emitter into a portable cooler module. We are in the process of mounting a SiC THz emitter onto a Stirling cycle cooler as shown in Fig. 11. This cooler has a capacity of 2.5 Watt at 80 K. The status of this work is that a vacuum shroud with a TPX transparent window is being machined to attach to the cold finger, which holds the emitter. Initial tests indicated that there was a vacuum leak, so the shroud is being reworked.


(a)

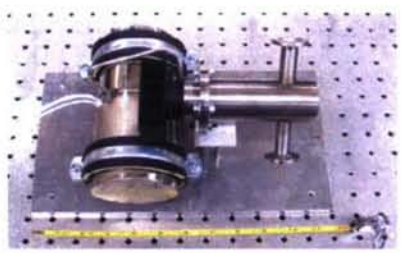

(b)

Figure 15. A picture of the AIM (AEG INFRAROT-MODULE GmbH) SL200 Cryogenic Linear Drive Stirling Cooler that we are using to develop a portable THz source. The cold finger is the lower-left small cylinder that will be mounted inside an evacuated chamber to avoid frost. The THz beam emits from a transparent TPX window. Overall size is about 10 cm on a side. Right panels show the cooler on an optical bench at the University of Delaware.

Laser Gain Calculations

Terahertz laser gain investigation.
A spherical cavity was suggested by Miron Kagan to obtain lasing in our resonant state laser.
We have analyzed of the gain of a silicon resonator and will show that lasing is possible in these structures. The electric field of a wave transmitted through a double-cleaved laser bar of length L, assuming perfect overlap between the gain region and optical mode, is

$$E_{tran} = \frac{(1-R)e^{ikL}}{1-Re^{2ikL}}, \qquad (1)$$

where R is the reflectivity of one facet, and

$$k = i\frac{\omega}{c}(n_{real} + in_{imag}), \qquad (2)$$

is the transmission coefficient. A positive imaginary index corresponds to loss; and negative to gain. Normally, we assume the imaginary component of the index is small compared to the real part (small gain or loss) and can equate:

$$n_{real} \cong n, \qquad (3)$$

where n_{real} is the lossless refractive index of the semiconductor, and n_{imag} is determined by:

$$\frac{2\omega n_{imag}}{c} = \alpha - \gamma, \qquad (4)$$

where α is the loss in the absence of any gain mechanism, and γ is the material gain in the presence of optical or electrical pumping. If the denominator of Eqn. (1) is zero, the infinite system gain will produce light output without an input wave, i.e. lasing. So, setting the denominator of Eqn. (1) to zero,

$$Re^{2ikL} = 1 \text{ (condition for oscillation or lasing).} \qquad (5)$$

Plugging in for k,

$$Re^{i(2\omega/c)L(n_{real}+in_{imag})} = 1 \qquad \text{(condition for lasing).} \qquad (6)$$

This complex equation has both real and imaginary parts:

$$e^{2i\omega Ln_{real}/c} = 1, \text{ or,} \qquad L = m\lambda/2, \qquad (7)$$

where λ is the wavelength within the material, m is an integer, and

$$Re^{(\gamma-\alpha)L} = 1. \qquad (8)$$

For silicon, $n \cong 3.5$, or $R \cong 0.31$. Thus, for silicon with cleaved facets, the lasing condition is

$$(\gamma-\alpha)L = 1.17 \qquad \text{(both facets cleaved, no coatings)} \qquad (9)$$

For a bar laser in which the reflectivities of the two facets are different, the gain condition is

$$2(\gamma-\alpha)L=\ln(1/R_1R_2). \quad \text{(both facets cleaved, with coatings)} \qquad (10)$$

If one of the facets is totally internally reflecting due to angled etching, the gain condition is

$$2(\gamma-\alpha)L=\ln(1/R_1). \quad \text{(TIR, one facet)} \qquad (11)$$

Figure 16 shows the gain of the active region that is required for lasing. A typical quantum cascade laser has a gain coefficient γ in the range from 50 to 70 cm^{-1}. Miron Kagan suggested that our SiGe resonant state devices have gain over twice this value. Assuming, conservatively, that our gain is 70 cm^{-1}, we should be able to achieve lasing if the cavity length exceeds 300 μm (from Fig. 15 (b) if we use a spherical resonator with total internal reflection, which is what we propose to do. We need to determine the dependence of gain on applied current density.

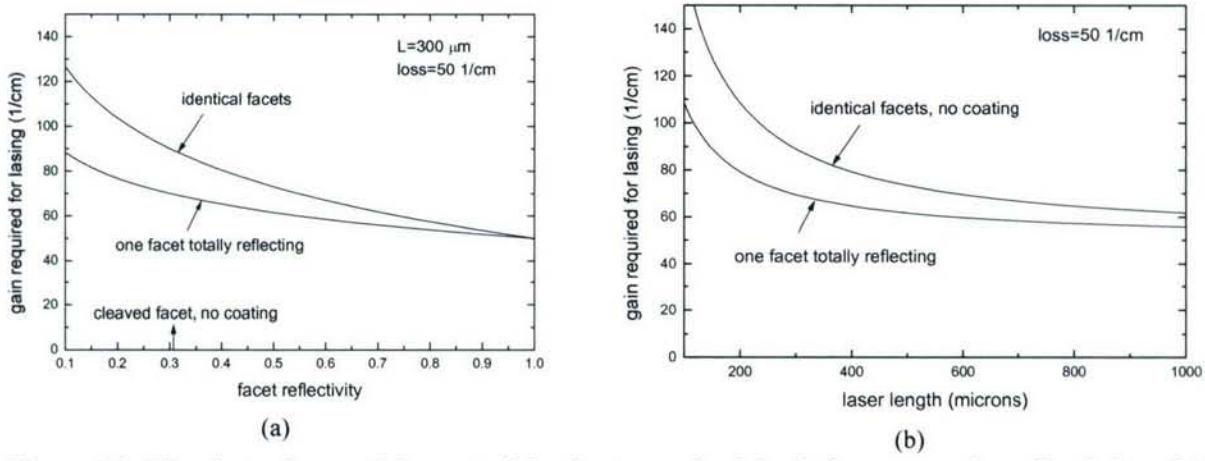

(a) (b)

Figure 16. The dependence of the material gain, γ, required for lasing versus the reflectivity of the facets for cavity length 300 um (left panel); and versus the cavity length for mirror reflectivity R=0.31 (right panel). Each graph above show curves for the two cases of: (1) identical facets; and (2) one facet is 100% reflecting (by TIR).

The rate of change in the density of excited impurities in the two-state system is given by:

$$\frac{\partial N^*}{\partial t}=\frac{\sigma J}{q}\left(N-N^*\right)-\frac{N^*}{\tau}=0$$

where J is the current density, σ is a capturing cross section for exciting impurities, q is the electronic charge, N is the doping concentration, N^* is the density of excited impurities, τ is the lifetime of the excited state, and η is the fraction of transitions leading to the emission of a photon.

The emitted power becomes:

$$P = \frac{\eta \hbar \omega_0 VN}{\tau} \times \frac{\frac{\sigma J \tau}{q}}{1 + \frac{\sigma J \tau}{q}}$$

For small currents, the output power is approximately:

$$P = \frac{\eta \sigma \cdot \hbar \omega_0 \cdot VN}{q} \cdot J$$

Terahertz Source Comparison

The devices fabricated and characterized at the University of Delaware have excellent properties as shown in the summary plot in Figure 1.

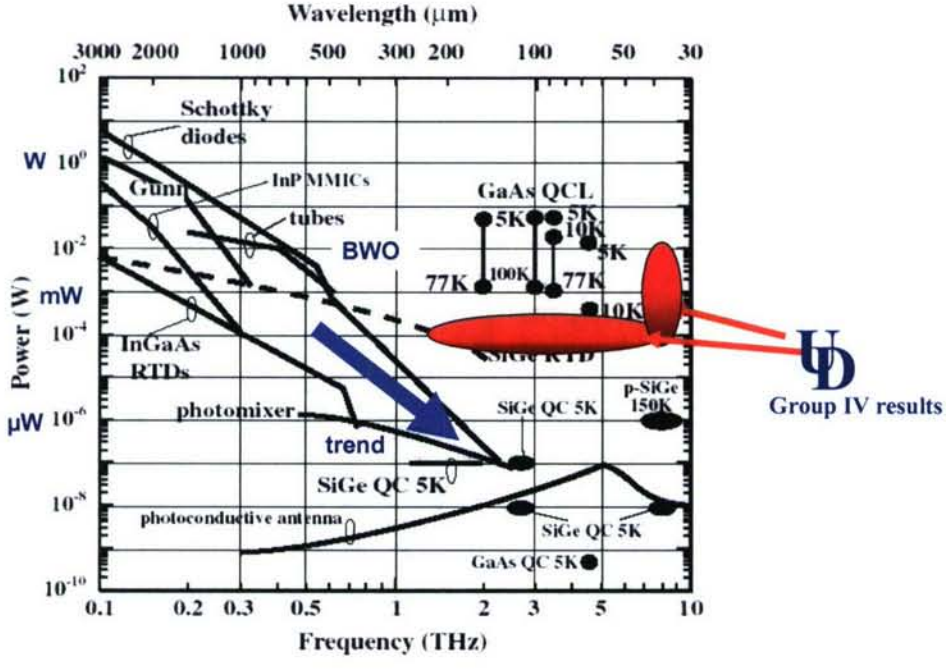

Figure 17. Graph above shows that the Univ. of Delaware (UD) has the highest power of all group IV sources: THz goals: compact, efficient, without using liquid cryogens.

4.2 THz Detectors and Imagers

Figure 18 shows the demonstration of Terahertz photocurrent from a Si based dopant based detector.

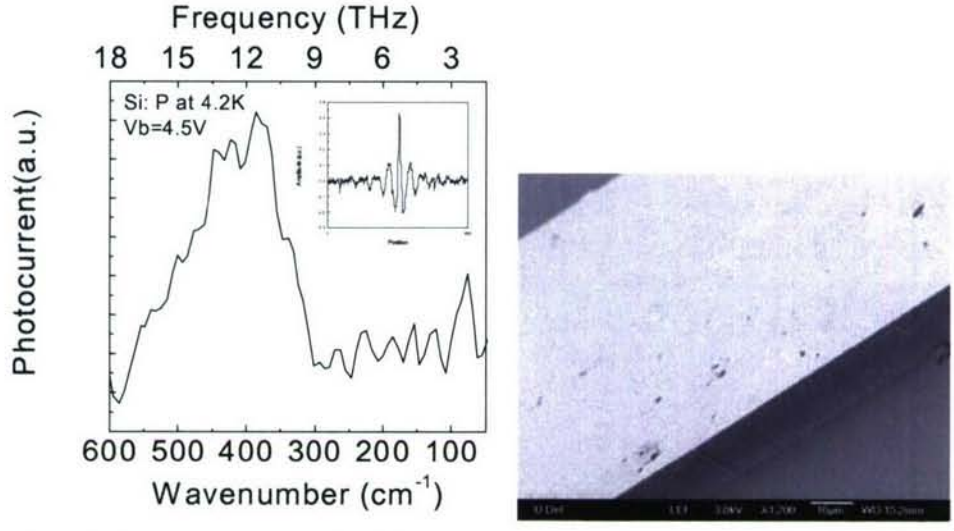

Figure 18. An example of Terahertz detection by phosphorus doped silicon devices. Left plot shows Spectral response of photocurrent versus wavenumber for Si-based THz detector at temperature of 4 K. The inset shows the interferogram of the detected signal measured by the FTIR spectrometer, indicating that the measurement is accurate. Right panel shows SEM micrograph of fabricated mesa detector with step height of 10 microns.

4.3 THz device characterization techniques

For source and detector characterization, we use a Fourier Transform Infrared Spectrometer (ThermoNicolet 780) as shown in Fig. 18.

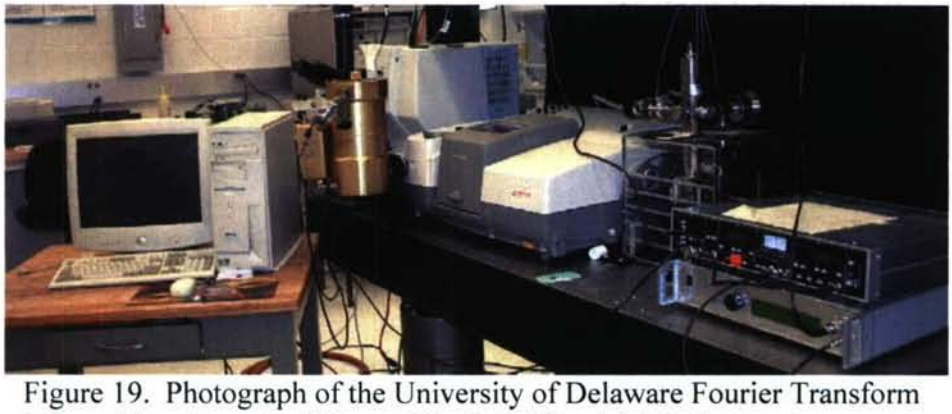

Figure 19. Photograph of the University of Delaware Fourier Transform Infrared Spectrometer (ThermoNicolet 780), which is the two-tone gray instrument in the center. To the left, the large gold colored cylinder attached to the FTIR is the silicon bolometer detector. To the right of the FTIR is the Plexiglas box containing the device cryostat (detail in Fig. 19).

(a) (b) (c)

Figure 20. Sample mounting techniques for low temperature emission characterization by FTIR. Left panel shows the sample mounting region inside the He-cooled cryostat. We use transmission windows made of either CsI (visually transparent), or, polyethylene (visually cloudy but more transmissive to THz). Middle panel shows a close-up view of the Cu mounting block with 3 samples, with fine gold wire bonds and heavier electrical contact wires. Right panel shows a THz device mesa with Au wire bonds.

4.4 Terahertz Properties of Materials

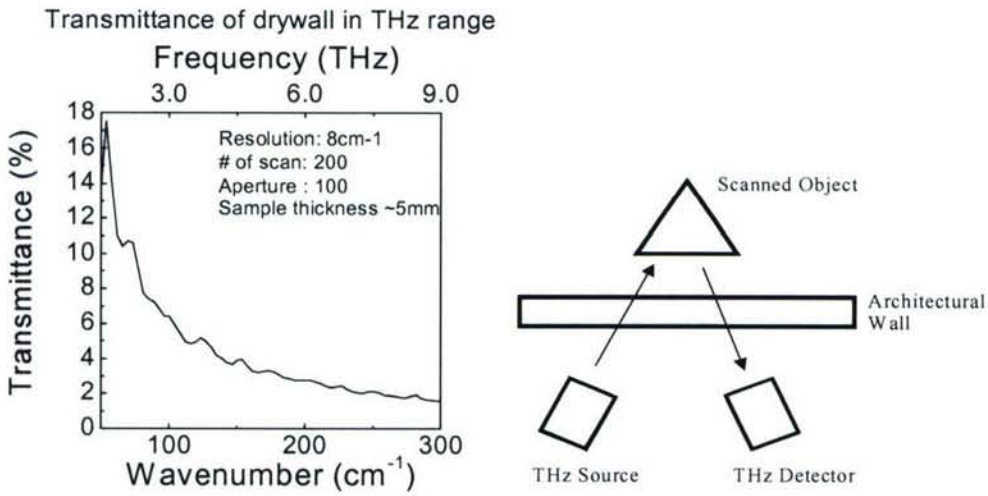

Figure 21. Example of penetration imaging in the terahertz range. Left plot shows measurement of transmission through architectural drywall (Sheetrock), demonstrating feasibility of THz penetration scanning. The transmittance above 1 % is sufficient for THz imaging using sources with output powers in the 100 microwatt range, and with available detectors. Right panel shows concept of terahertz refection imaging through object.

Terahertz penetration imaging through architectural drywall

We attempted to understand the propagation of THz frequencies through scattering material, particularly architectural drywall or Sheetrock, which is largely hydrated $CaSO_4$. There was recently some controversy regarding whether THz can, or cannot penetrate drywall. We have found that frequencies below 3 THz can penetrate standard thickness, and we are preparing a monograph on this topic. Our modeling approach is to use a theory of diffusion in which the photons are making a

random walk through the material and hence "diffusing" through the medium. We derived the following equation:

$$T = \frac{Ac(1+B)/\nu}{L+2ABc/\nu} = \frac{A(1+B)}{(L/c)\nu+2AB}$$

where A and B are fitting parameters, ν is the frequency, and L is the thickness and c is the speed of light. The following plot is transmission though 5 mm thick drywall taken here at UDel.

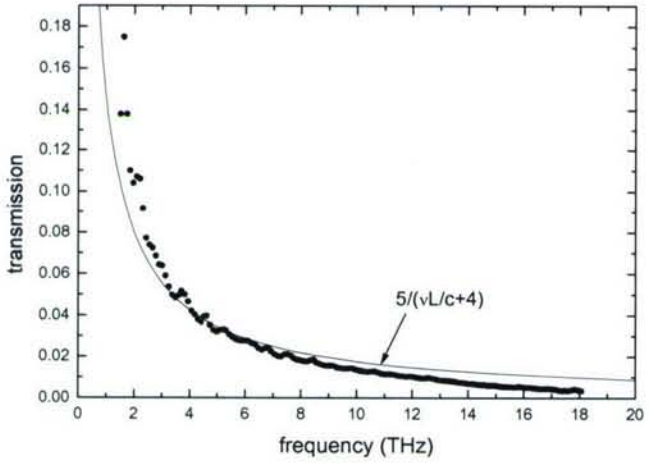

Figure 22. Plot of transmission though 5 mm thick drywall, taken here at UDel. Also shown is the best fit using a theory of photon diffusion. We are attempting to adjust the parameters to improve the fit, and to understand the transmission process.

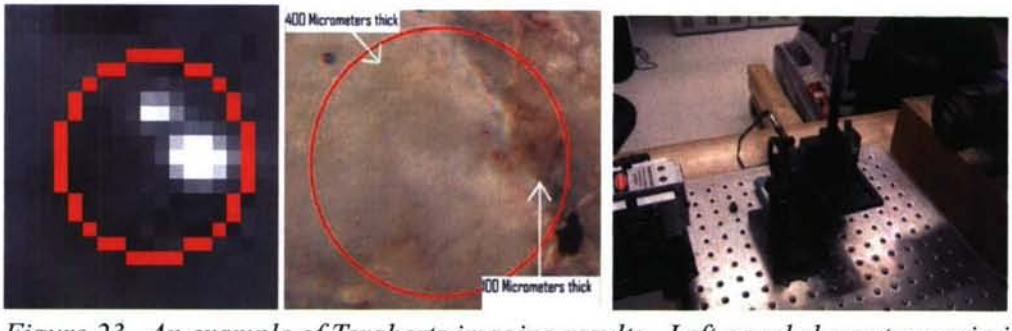

Figure 23. An example of Terahertz imaging results. Left panel shows transmission picture of a thin bone sample taken with terahertz camera. Middle panel shows visible light photograph of same bone, showing that THz reveals thickness variations. Right panel shows the THz camera system

Electrically Alterable Photonic Crystals

An electrically controlled diffractive element can be produced by changing the conductivity in a relatively intrinsic region of silicon by carrier injection. This would give the region control over the effective skin depth, which is the penetration of the incident electromagnetic energy. This electrically

controlled diffractive element was realized by using a p-i-n diode structure. The p and n regions would be interdigitated with the intrinsic region in between. When the diode is forward biased or under high reverse bias (under breakdown conditions) carriers will injected into the intrinsic region from the n and p regions. The number of carriers in the intrinsic region will change the conductivity, hence the apparent skin depth will also change. Carriers will change the dielectric properties and allow phase control of the energy passing through the region, which will affect the transmission of the diffraction grating.

An electrically controlled grating could also be used in optical switching devices by steering the incoming optical beam to the desired optical output channel at microwave switching speeds, which could have applications in telecommunications equipment and optical computers. To make an electrically active device, we fabricated a structure and have been characterizing it. Changes were observed in transmittance and reflectance, but we are evaluating if these changes are due to the plasma dispersion effect or to heating.

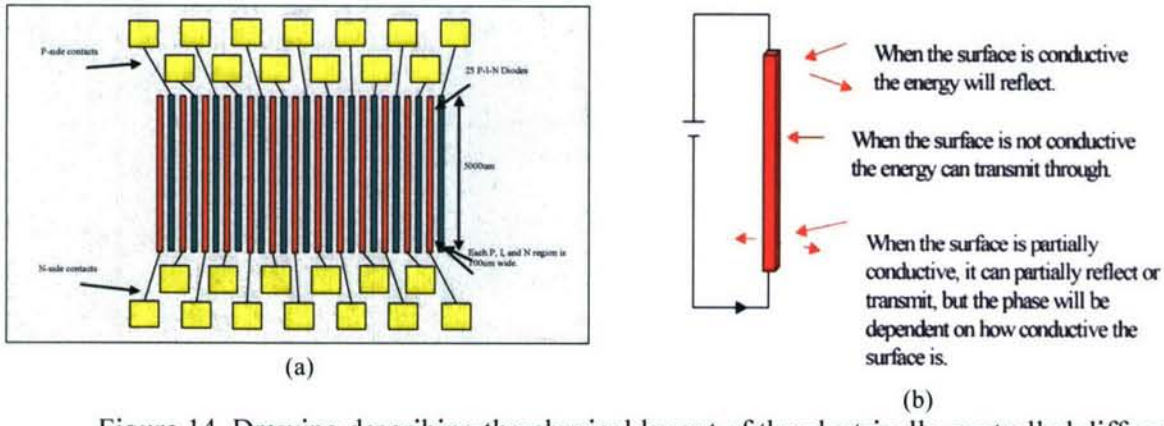

(a) (b)

Figure 14. Drawing describing the physical layout of the electrically controlled diffractive grating. Right panel shows the operation of the device.

Active Terahertz Imaging Solid State Imaging at 77 K: 2-dimensional Si:Ga top-emitter arrays with long wavelength HgCdTe photoconducting detectors

We developed an active "T-Ray" imaging system using compact components. The 12-14 THz emission band of Ga-doped silicon devices, combined with long-wavelength, highly sensitive HgCdTe ("MCT") detectors for operation at 77K, allow simple, non-liquid helium-based cooling. This system allows portable see- through material imaging systems. Long-wavelength MCT detectors just overlap with the spectrum of Ga-doped Si emission, enabling imaging at 13 THz.

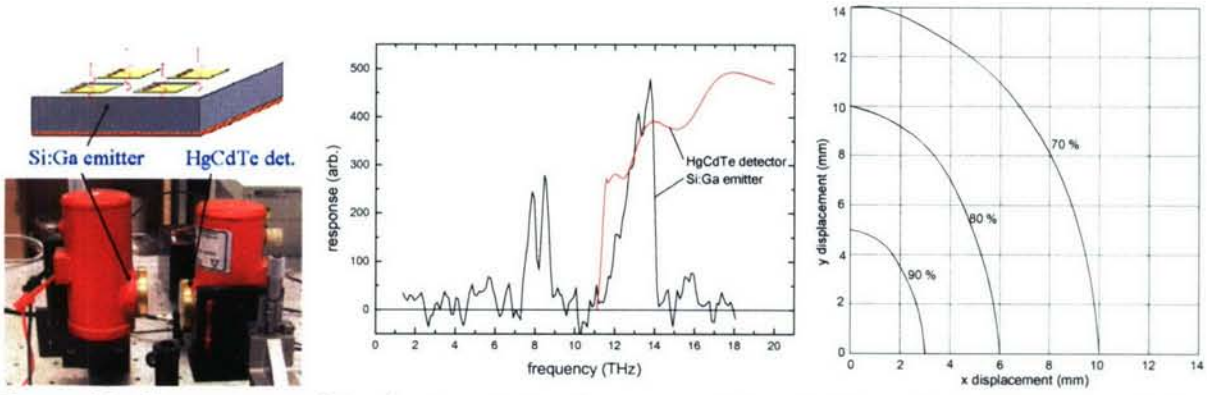

Figure 25. Comparison of Terahertz emission from several doped silicon devices. Left panel shows THz beam generation and detection with the Si:Ga emitter and HgCdTe ("MCT") detector. Middle panel shows the overlap in wavelength of the long-wavelength MCT detectors with the Ga-doped Si emission, enabling imaging at 13 THz. Right panel shows the near field intensity pattern that was measured for the emitter at a distance of 8 cm; ~indicating 15° beam divergence.

Although the long-wavelength photoconducting HgCdTe detector is not available in arrays, we can produce the THz surface *emitters* in arrays, and so by sequentially turning on each element in the emitter array, and using a single detector, we should be able to construct an image without mechanical movement. Ultimately, this time-sequenced emitter array can be integrated with the activating circuitry, allowing a compact solid state imaging system.

The next research steps are to: (a) Insert optics to obtain a collimated beam and begin raster scanned imaging as in T-Ray imaging. (b) Produce Si:Ga addressable array to allow non-mechanical sequential image formation using emitter array and single detector (MCT photoconductors are not available in arrays). (c) Develop circuitry for sequential emitter activation that will allow automatic, rapid solid state imaging at 13 THz and 77 K.

Etching Techniques Developed to Fabricate Photonic Crystals

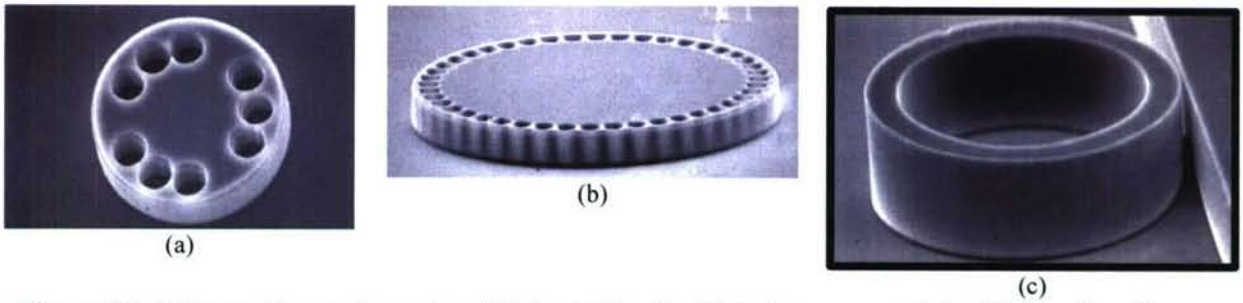

Figure 26. Waveguides and couplers fabricated by the Kolodzey group at the University of Delaware.

Technology transitions and collaborations

Technology transitions included discussions and meetings regarding terahertz nanotechnology with Smiths Heimann Corp., IBM Corporation, and with Intelligent Automation Inc (IAI), a small business in Rockville, MD. We established vigorous collaboration with the Army Night Vision Lab to develop components and techniques for THz imaging systems using Stirling cycle coolers, and bolometer detector array.

Figure 27. Photo of the Chemical Vapor Deposition System (Unaxis CVD300) being installed in room 105 DuPont Hall at the University of Delaware. This system was donated by IBM Corporation and will be used to fabricate infrared detectors based on SiGe quantum dots and nanostructures.

4.5 Relevance and impact of the Accomplishments

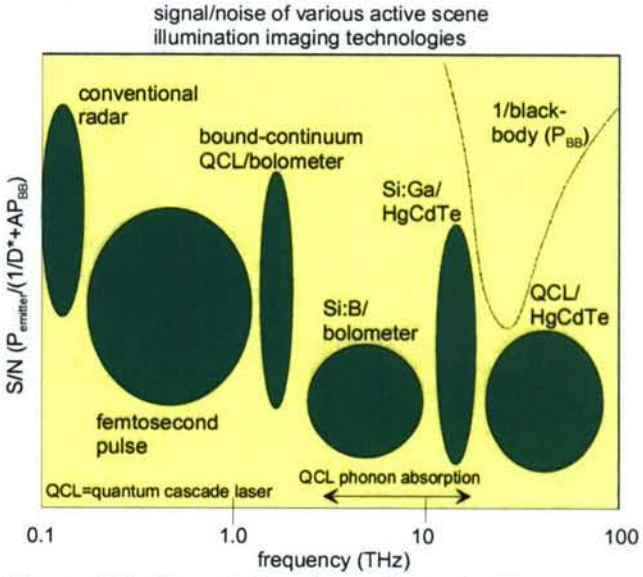

Figure 28. Plot of signal to noise ratio for source/detector combinations over different spectral ranges, showing advantages of Active Terahertz Imaging compared to other technologies

Electrically pulsed Terahertz emitting devices were fabricated from p-type and n-type doped silicon, and were measured by Fourier Transform spectroscopy. Terahertz emitting devices that are electrically pumped, and that can be fabricated by conventional processing compatible with integrated circuits, are important for many applications in the areas of penetration ranging thorough architectural walls, short distance wide band communications, biochemical identification, detection of explosives and metals, and for medical diagnostics. A THz laser may be feasible using the dopant approach. Due to the limitations and high absorption of competing materials, the SiGe based THz emitters are the only reasonable technology in the range from 4 to 25 THz. The emitting and detecting devices described here are highly relevant to the AFOSR mission by providing integrated nanoscale THz emitters and detectors that can be incorporated into arrays, and serve dual use for commercial products. These results indicated the directions and approaches that can enable THz systems compatible with silicon technology and that can be further investigated with DOD Lab collaboration.

Specific examples of scientific progress include: (1). achieved high power, higher temperature emission from doped silicon, SiGe, SiC and GaAs; (2) optimized and clarified the mechanism of THz emission by dopant emission for maximum gain; (3) demonstrated that impurity based devices can emit THz at least up to temperatures of 150 K; (4) fabricated and tested laser structures; investigate emission from delta doping devices for tunable emission; and (5). that THz detectors based on superlattices, dopant devices and from HgCdTe can operate at 77 K for portable THz systems.

- Sources-
  - Conventional millimeter wave radar works to ~ 0.2 THz.
  - Femtosecond generation of THz works to ~ 2 THz.
  - Quantum cascade lasers have two windows at 2-4 THz and 25-100 THz with nothing in between.
  - The doped silicon emitters developed here operate in the 4-25 THz gap.

- Detectors-
  - Bolometers work over any range with ~ 1 nW NEP.

- HgCdTe works > 12 THz with 0.1 nW NEP.
- Thermal noise peaks at 30 THz, drops significantly by 15 THz.
- Si:Ga emitters with HgCdTe detectors in the 12-15 THz range offer great potential for active imaging.

In the 4 to 25 THz range, doped silicon emitters are the only source technology. They can be used with bolometers and with HgCdTe detectors. This THz range provides strong resonance with biochemicals for identification

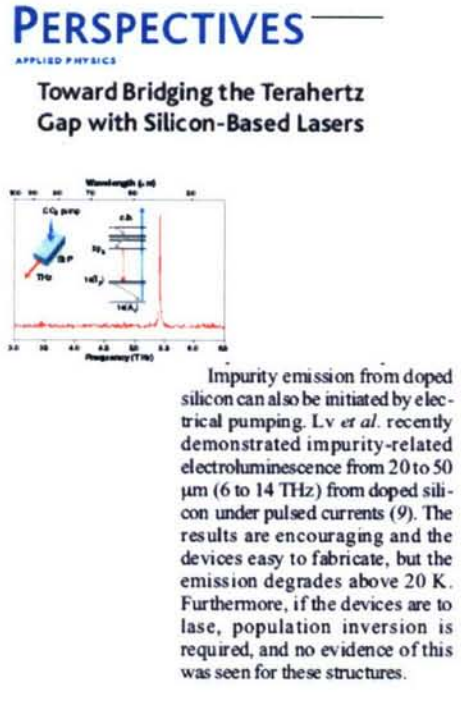

PERSPECTIVES

APPLIED PHYSICS

Toward Bridging the Terahertz Gap with Silicon-Based Lasers

Impurity emission from doped silicon can also be initiated by electrical pumping. Lv *et al.* recently demonstrated impurity-related electroluminescence from 20 to 50 μm (6 to 14 THz) from doped silicon under pulsed currents (*9*). The results are encouraging and the devices easy to fabricate, but the emission degrades above 20 K. Furthermore, if the devices are to lase, population inversion is required, and no evidence of this was seen for these structures.

29 APRIL 2005 VOL 308 SCIENCE www.sciencemag.org

Figure 29. Reprint of story about our work at the University of Delaware that is cited by the journal, Science, in a review on THz.

5. Personnel Supported with the research effort:

Faculty:
James Kolodzey
Keith Goossen

Graduate Students:
Pengcheng Lv (Kolodzey)
Paola Murcia (Goossen)
Nate Sustersic (Kolodzey)
Paola Murcia (Goossen)

Post Doc:
Pengcheng Lv (Kolodzey)

6. Publications:

M. S. Kagan, I. V. Altukhov, E. G. Chirkova, V. P. Sinis, R. T. Troeger, S. K. Ray, and J. Kolodzey, "THz lasing of SiGe/Si quantum-well structures due to shallow acceptors," Phys. Stat. Sol., v. (b) 235, no. 1, pp. 135-138, 2003.

M. S. Kagan, I. V. Altukhov, E. G. Chirkova, V. P. Sinis, R. T. Troeger, S. K. Ray, and J. Kolodzey, "THz lasing due to resonant acceptor states in strained p-Ge and SiGe quantum-well structures," Phys. Stat. Sol., v. (b) 235, no. 2, pp. 293-296, 2003.

Shouyuan Shi, Dennis W. Prather, Liuqing Yang, and James Kolodzey, "Influence of support structure on microdisk resonator performance," Optical Engineering, v. 42, Number 2, pp. 383-387, 2003.

T. N. Adam, R. T. Troeger, S. K. Ray, P.-C. Lv, and J. Kolodzey, "Terahertz electroluminescence from boron impurities in bulk silicon," Appl. Phys. Lett., vol. 83, (9), pp. 1713-1715, 2003.

Kagan MS, Altukhov IV, Sinis VP, Chirkova EG, Yassievich IN, Kolodzey J, "Terahertz stimulated emission from strained p-Ge and SiGe/Si structures," Journal Of Communications Technology And Electronics, v. 48 (9), pp. 1047-1054 Sep. 2003.

Sriram Venkataraman, Janusz Murakowski, Thomas N. Adam, James Kolodzey, Dennis W. Prather, "Fabrication of high-fill-factor photonic-crystal devices on silicon-on-insulator substrates (JM3 073007)," J. Microlithography, Microfabrication, and Microsystems, v. 2, number 4, pp. 248–254, October 2003.

I.V. Altukhov, E.G. Chirkova, V.P. Sinis, M.S. Kagan, R.T. Troeger, S.K. Ray, J. Kolodzey, A.A. Prokofiev, M.A. Odnoblyudov, I.N. Yassievich, "Effect of potential and doping profiles on excitation of stimulated THz emission of SiGe/Si quantum-well structures," Physica B-Condensed Matter, v. 340-342, pp. 831-834, Dec 31 2003.

P.-C. Lv, R. T. Troeger, T. N. Adam, S. Kim, J. Kolodzey, I. N. Yassievich, M. A. Odnoblyudov, and M. S. Kagan, "Electroluminescence at 7 terahertz from phosphorus donors in silicon," Appl. Phys. Lett., vol. 85, (1) pp. 22-24, 2004.

P.-C. Lv, R. T. Troeger, S. Kim, S. K. Ray, K. W. Goossen, and J. Kolodzey, I. N. Yassievich, M. A. Odnoblyudov, and M. S. Kagan, "Terahertz emission from electrically pumped gallium doped silicon devices," Appl. Phys. Lett., v. 85 (17), pp. 3660-3662, 2004.

J. Kolodzey, T. N. Adam, R. T. Troeger, P.-C. Lv, S. K. Ray, I. Yassievich, M. Odnoblyudov, and M. Kagan, "Terahertz emitters and detectors based on SiGe nanostructures," International Journal of

Nanoscience, vol. 3, nos. 1 & 2, pp. 171-176, 2004.

S. K. Ray, T. N. Adam, R. T. Troeger, J. Kolodzey, G. Looney, and A. Rosen, "Characteristics of THz waves and carrier scattering in boron-doped epitaxial Si and Si1-xGex films," Journal Appl. Phys., vol. 95, pp. 5301 – 5304, May 2004.

"Surface terahertz emitter based upon impurity transitions," P. Salazar and K.W. Goossen, 2004, in press.

I. V. Antonova, V. I. Obodnikov, M. S. Kagan, R. T. Troeger, S. K. Ray and J. Kolodzey. Capacitance study of selectively doped SiGe/Si heterostructures. Semicond. Sci. Technol., v. 20, 335, 2005.

I.V. Antonova, M.S. Kagan, V.I. Polyakov, L.L. Golik, J. Kolodzey, Effect of interface states on population of the quantum wells in SiGe/Si structures, Physica Status Solidi (C), v. 2, (6), pp. 1924-1928, April 2005.

P. –C. Lv, X. Zhang, and J. Kolodzey, M. A. Odnoblyudov, and I.N. Yassievich, "Tunable terahertz emission from phosphorus doped silicon under uniaxial compressive stress," J. Appl. Phys., v. 98, 103511, 2005.

P. –C. Lv, R. T. Troeger, X. Zhang, T. N. Adam, J. Kolodzey, M. A. Odnoblyudov, and I.N. Yassievich, "Hot hole redistribution in impurity states of boron doped silicon terahertz emitters," J. Appl. Phys., v. 98, 093710, 2005.

P. –C. Lv, X. Zhang, A.R. Powell, and J. Kolodzey, "High- temperature impurity based terahertz emitters: nitrogen doped 4H- SiC devices," Appl. Phys. Lett., v. 87, 241114, 2005.

James Kolodzey, Pengcheng Lv, S. Ghosh, P. Pellegrini and G. Xuan, "Use of terahertz technology for spectroscopic detection of concealed weapons from stand off ranges," SPIE Defense and Security Symposium (DSS),: Optics And Photonics In Global Homeland Security, Orlando, Florida, USA, 28 March – 1 April 2005; Proceedings of SPIE Vol. #5781-15. (invited talk)

7. Interactions/Transitions:

a. Participation/presentations at meetings, conferences, seminars, etc.

2006 Lester Eastman Conference, Cornell Univ., August 2-4, 2006, "Terahertz emission from electrically pumped SiGe intersubband devices," International Journal of High Speed Electronics and Systems.

"Terahertz Technology For Spectroscopic Stand-Off Detection Of Concealed Weapons," SPIE Global Homeland Security Technical Group Conference, 28 March – 1 April 2005, Orlando, Florida USA, (invited talk).

"High Power Terahertz Emission from Silicon Carbide Devices Operating at Temperatures up to 100 K," SURA 2005 Terahertz Applications Symposium, Southeastern Universities Research Association, June 2-3, 2005, (invited talk)

"Terahertz Technology for Remote Sensing and Identification," Army Research Night Vision Lab, Ft. Belvoir, VA, 21 July 2005, (invited talk).

"Terahertz Devices and Spectroscopy," Detecting Illicit Substances: Explosives & Drugs, Gordon Research Conferences, August 28 - September 2, 2005, Les Diablerets, Switzerland, (invited talk).

"Terahertz Devices for Imaging and Sensing," Boston IEEE-LEOS Terahertz Workshop, MIT Lincoln Labs, 19 October 2005, (invited talk).

Twelfth International Workshop on The Physics of Semiconductor Devices 16-20 Dec., 2003, Chennai, India. (invited talk)

National Laser Symposium 2003, 22-24 Dec., 2003, Kharagpur, India. (invited talk)

2004 International Microwave Symposium, Fort Worth, Texas, June 6-11, 2004, IMS2004 Technical Digest.

First IEEE International Conference on Group IV Photonics, Hong Kong, 29 Sept. 2004. (invited talk)

12th International Symposium on Ultrafast Phenomena in Semiconductors, Vilnius, Lithuania, 22 Aug. 2004, (invited talk)

SPIE Optics East Conference on Semiconductor and Nanotechnologies and Applications; Nanosensing: Materials and Devices, Philadelphia, 25–28 October 2004; (invited talk)

2004 Lester Eastman Conference, Rensselaer Polytechnic Institute, August 4-6, 2004, International Journal of High Speed Electronics and Systems.

6th International Conference on Mid-Infrared Optoelectronic Materials and Devices, St Petersburg, June 28 -- July 02, 2004.

2004 IEEE LEOS Annual Meeting, Conference Proceedings, 7-11 November 2004, Westin Rio Mar Beach, Rio Grande, Puerto Rico (invited talk on Arrayed Optoelectronic Modules)

b. Consultative and advisory functions to other laboratories and agencies.
During the course of this program, the following interactions took place:

Miron Kagan (IRE, Russian Academy of Science, Moscow); Irina Yassievich and Maxim Odnoblyudov (Ioffe Institute, St. Petersburg)

Collaboration with Dr. Tom Allik of the Army Night Vision Laboratory, Ft. Belvoir, VA

Collaboration with Dr. Tom Adam of the IBM Corporation, Watson Research Center, Yorktown Heights, NY.

The acquisition of a SiGe CVD deposition system (Unaxis CVD300) from IBM Corporation

SBIR contract with Dr. Eric van Dorn of Intelligent Automation Inc (IAI), Rockville, MD.

Scott Simon of University of Pennsylvania medical school for bone scans

Greg Gonye of Thomas Jefferson Medical School in Philadelphia for THz properties of DNA.

Meetings with engineers from W.L. Gore & Associates regarding THz device products

Judson Technologies has provided an MCT detector for THz imaging

c. Transitions. cases where knowledge resulting from effort is used:

Discussions on terahertz imaging and sensing with Dr. K. Roe of Smiths Detection Corp., manufacturer of x-ray scanners for airports, Dr. Gwyn Williams of Jefferson Lab for high power THz sources, and Claire Gmachl for THz emitting devices.

8. New discoveries, inventions, or patent disclosures.

2 patents:

1. Terahertz Frequency Radiation Sources And Detectors Based On Group Iv Materials And Method Of Manufacture, J. Kolodzey, S. Ray, T. Adam, P. Lv, T. Troeger, M. Kagan, I. Yassievich, M. Odnoblyudov, (Ser. No. 60/461,656), Filed April 9, 2004.

2. Terahertz Frequency Band Wavelength Selector, J. Kolodzey, T. Adam, D. Prather, (Ser. No. 10/820,517), Filed April 8, 2004.

9. Honors/Awards:

James Kolodzey received the IBM Faculty Award, with $20,000, to study semiconductor dopants in nanostructures to improve the performance of integrated circuits for future computers. (http://www.udel.edu/PR/UDaily/2006/nov/kolodzey111405.html)

James Kolodzey was appointed the Charles Black Evans Professor in Electrical Engineering in recognition of scholarship, teaching and service to the University of Delaware, Oct. 1, 2004, (http://www.udel.edu/PR/UDaily/2005/oct/namedprof100104.html)

10. Markings:

In order to ensure prompt receipt and acceptance, mark the outside of the package clearly to indicate that it is a performance report.